



Supporting Online Material for

Tryptophan-Accelerated Electron Flow through Proteins

Crystal Shih, Anna Katrine Museth, Malin Abrahamsson,
Ana Maria Blanco-Rodriguez, Angel J. Di Bilio, Jawahar Sudhamsu,
Brian R. Crane,* Kate L. Ronayne, Mike Towrie, Antonín Vlček, Jr.,*
John H. Richards,* Jay R. Winkler,* Harry B. Gray*

*To whom correspondence should be addressed. E-mail: bc69@cornell.edu (B.R.C.);
a.vlcek@qmul.ac.uk (A.V); jhr@caltech.edu (J.H.R.); winklerj@caltech.edu (J.R.W.);
hbgray@caltech.edu (H.B.G.)

Published 27 June 2008, *Science* **320**, 1760 (2008)
DOI: 10.1126/science.1158241

This PDF file includes:

Materials and Methods
Figs. S1 to S3
Table S1
References

SUPPORTING MATERIAL

Materials and Methods

Preparation of $\text{Re}^{\text{I}}(\text{CO})_3(\text{dmp})(\text{H}^{124})/(\text{W}^{122})/\text{AzCu}^{\text{I}}$

Mutant azurins were expressed and $\text{Re}^{\text{I}}(\text{CO})_3(\text{dmp})(\text{H}^{124})/(\text{W}^{122})/\text{AzCu}^{\text{I}}$ was prepared using previously published protocols (S1,S2).

Crystal Structure of $\text{Re}^{\text{I}}(\text{CO})_3(\text{dmp})(\text{H}^{124})/(\text{W}^{122})/\text{AzCu}^{\text{II}}$

Crystals of $\text{Re}(4,7\text{-dimethyl-1,10-phenanthroline})(\text{CO})_3(\text{H}^{124})\{\text{T}^{124}\text{H}|\text{K}^{122}\text{W}|\text{H}^{83}\text{Q}\}(\text{Cu}^{\text{II}})\text{-azurin}$ ($\text{Re}^{\text{I}}(\text{CO})_3(\text{dmp})(\text{H}^{124})/(\text{W}^{122})/\text{AzCu}^{\text{II}}$; space group I222, cell dimensions $63.22 \times 69.08 \times 68.94 \text{ \AA}^3$; $\alpha = \beta = \gamma = 90.00^\circ$, one molecule per asymmetric unit) grew from 4 μL drops made from equal volumes of 30 mg/mL $\text{Re}^{\text{I}}(\text{CO})_3(\text{dmp})(\text{H}^{124})/(\text{W}^{122})/\text{AzCu}^{\text{II}}$ in 25 mM HEPES pH 7.5 and reservoir by vapor diffusion. The drops were equilibrated against 500 μL of reservoir containing 20-24% PEG molecular weight 4000, 100 mM LiNO_3 and 100 mM citric acid pH 3.2. Diffraction data (30.0-1.50 \AA resolution, 99.6% complete, $R_{\text{Sym}} = \sum \sum_j |I_j - \langle I \rangle| / \sum \sum_j I_j = 8.2\%$; overall signal-to-noise = $\langle I/\sigma I \rangle = 34.4$) were collected on a Quantum-210 CCD (Area Detector Systems Corporation), at the Cornell High Energy Synchrotron Source, beamline A1 (0.972 \AA) and processed with HKL2000 (S3). The structure was determined by molecular replacement with AmoRe (S4) using a probe derived from the structure of azurin (PDB code: 1BEX). Rigid-body, positional and thermal factor refinement and adding water molecules and $\text{Re}(\text{dmp})(\text{CO})_3$ with CNS (S5) amidst rounds of manual rebuilding with XFIT (S6) produced the final model (1.50 \AA resolution, R-free = 25.5%, R-factor = 23.6%). The refinement was performed against all but 5% of the reflections, which were used to calculate an R-free value. The crystallographic distances between the redox-active centers are as follows: $\text{Cu-W}^{122} = 11.1 \text{ \AA}$, $\text{W}^{122}\text{-Re} = 8.9 \text{ \AA}$, $\text{Cu-Re} = 19.4 \text{ \AA}$. Data collection and refinement statistics are listed in Table S1.

Time-Resolved Spectroscopy

TRIR. The ps-TRIR experiments were carried out at the Central Laser Facility of the Rutherford Appleton Laboratory, UK. This apparatus has been described in detail previously (S7,S8). Briefly, part of the output from a 1 kHz, 800 nm, 150 fs, 1 mJ Ti-Sapphire oscillator/regenerative amplifier (Spectra Physics Tsunami/Spitfire) was used to pump a white light continuum seeded β -barium borate (BBO) OPA. The signal and idler produced by this OPA were difference frequency mixed in a type I AgGaS₂ crystal to generate tunable broadband midinfrared pulses (ca. 150 cm⁻¹ FWHM, 0.1 μ J), which were split to give probe and reference pulses. The probe pulses were focused into the sample and imaged onto the input slit of a spectrograph (150 lines/mm). The reference pulses followed a similar optical path but were transmitted through a cell containing only the solvent and then imaged into a second spectrograph. For experiments in the 1-2000 ps time range, second harmonic generation of the residual 800 nm light provided 400 nm pump pulses (~150 fs FWHM, 3 μ J), which were sent along a delay line before exciting the sample at magic angle. Both the pump and probe pulses were focused to a diameter of 200-300 μ m at the sample. Changes in infrared absorption at various pump-probe time delays were recorded by normalizing the outputs from a pair of 64-element HgCdTe (MCT) infrared linear array detectors on a shot-by-shot basis at 1 kHz. Data were collected in pump-on/pump-off pairs in order to minimize the effect of long-term drift in the laser intensity. The same equipment was used also in the nanosecond time domain. The sample was pumped by 355 nm, ~0.7 ns FWHM, ~3 μ J laser pulses generated by an actively switched AOT-YVO-20QSP/MOPA Nd:Vanadate diode-pumped microlaser, that was electronically synchronized with the femtosecond probe system (S8). The pump beam was set at a magic angle and focused to a diameter of 200-300 μ m at the sample.

Samples for TRIR measurements were prepared under a nitrogen atmosphere in a glove bag. Approximately 4 μ M solutions of $\text{Re}^{\text{I}}(\text{CO})_3(\text{dmp})(\text{H}^{124})[(\text{W}^{122})]\text{AzCu}^{\text{II}}$ in D_2O phosphate buffer (pH = 7.0) were reduced by slow dropwise addition of a D_2O phosphate buffer solution of sodium dithionite (Aldrich) until disappearance of the blue color. The reduced protein solution was placed in a custom-made (Harrick Scientific Corp.) IR solution cell equipped with CaF_2 windows, one of which with a drilled circular groove a 1 cm diameter and 75 μ m depth. The cell was rapidly oscillated in the plane perpendicular to the direction of the laser beams in order to minimize the potential build-up of decomposition products on the windows. The sample integrity was checked by FTIR spectra measured before and after each experiment.

Visible Transient Absorption. Samples were excited with the third harmonic (355 nm) from a Q-switched Nd:YAG laser (8 ns pulsewidth). Probe light was provided by a current-pulsed Xe arc lamp (500 nm), or a HeNe laser. Signal acquisition methods have been described previously (S9).

Luminescence. Samples were excited with the third harmonic from a regeneratively amplified passively mode-locked Nd:YAG laser (~15 ps pulsewidth). Luminescence was selected with a 420-nm longpass filter and detected using a picosecond streak camera operating in photon-counting mode (S10).

Kinetics Modeling

The kinetics model for electron tunneling in $\text{Re}^{\text{I}}(\text{CO})_3(\text{dmp})(\text{H}^{124})[(\text{W}^{122})]\text{AzCu}^{\text{I}}$ (**E**) is outlined in Figure S1. The decay of the initially formed singlet MLCT excited state ($^1\text{Re}^{\text{II}}(\text{CO})_3(\text{dmp}^{\bullet-})(\text{H}^{124})[(\text{W}^{122})]\text{AzCu}^{\text{I}}$) proceeds on a subpicosecond timescale and was not included in the model. Instead, it was assumed that a majority population of the vibrationally excited $^3\text{MLCT}$ state (**A**, 90%) and a minority population of the electron-transfer product $\text{Re}^{\text{I}}(\text{CO})_3(\text{dmp}^{\bullet-})(\text{H}^{124})[(\text{W}^{122})]^+\text{AzCu}^{\text{I}}$ (**C**, 20%) were present at $t = 0$. Vibrational cooling to yield

the thermally equilibrated $^3\text{MLCT}$ state (**B**) proceeds in competition with additional electron transfer producing **C**. The populations of **B** and **C** approach equilibrium, followed by electron transfer from Cu^{I} to produce $\text{Re}^{\text{I}}(\text{CO})_3(\text{dmp}^{\bullet-})(\text{H}^{124})[(\text{W}^{122})]\text{AzCu}^{\text{II}}$ (**D**).

The differential equations describing the kinetics of this model are:

$$\frac{d[A]}{dt} = -(k_1 + k_2)[A]$$

$$\frac{d[B]}{dt} = k_1[A] - (k_3 + k_7)[B] + k_4[C]$$

$$\frac{d[C]}{dt} = k_2[A] + k_3[B] - (k_4 + k_5 + k_8)[C]$$

$$\frac{d[D]}{dt} = k_5[C] - k_6[D]$$

Initial conditions are:

$$[A]_0 = 0.80 \quad [C]_0 = 0.20$$

Mass balance is given by:

$$[A]_0 + [B]_0 = [A] + [B] + [C] + [D] + [E]$$

The solution of this initial value problem is a quadruple-exponential function with observed rate constants λ_1 , λ_2 , λ_+ , and λ_- defined in terms of elementary specific rates as:

$$\lambda_1 = k_1 + k_2$$

$$\lambda_2 = k_6$$

$$\lambda_{\pm} = \frac{1}{2}(k_3 + k_4 + k_5 + k_7 + k_8) \pm \frac{1}{2}\sqrt{(k_3 + k_4 + k_5 + k_7 + k_8)^2 - 4(k_3 + k_7)(k_5 + k_8) - 4k_4k_7}$$

The rate constant $\lambda_2 = k_6$ describes the final step in the reaction sequence, the conversion of $\text{Re}^{\text{I}}(\text{CO})_3(\text{dmp}^*)(\text{H}^{124})|(\text{W}^{122})|\text{AzCu}^{\text{II}}$ into the ground-state resting species $\text{Re}^{\text{I}}(\text{CO})_3(\text{dmp})(\text{H}^{124})|(\text{W}^{122})|\text{AzCu}^{\text{I}}$. The value for this constant was extracted from fits to the microsecond timescale UV/vis and IR transient absorption data:

$$\lambda_2 = k_6 = 3.2 \times 10^5 \text{ s}^{-1} = (3.1 \text{ } \mu\text{s})^{-1}$$

Values of λ_1 , λ_+ , and λ_- were extracted from fits to the luminescence decay and TRIR kinetics.

Values of $k_7 = 7.7 \times 10^5 \text{ s}^{-1}$ and $k_8 = 2.0 \times 10^7 \text{ s}^{-1}$ were assigned on the basis of luminescence decay measurements in $\text{Re}^{\text{I}}(\text{CO})_3(\text{dmp})|(\text{F}^{122})|\text{AzCu}^{\text{I}}$ and TRIR measurements in $\text{Re}^{\text{I}}(\text{CO})_3(\text{dmp})(\text{H}^{124})|(\text{W}^{122})|\text{AzZn}^{\text{II}}$, respectively.

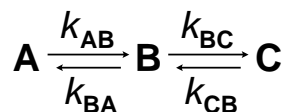
The ratio $k_3/k_4 = K = 3$ was determined from the amplitudes of the phases in the luminescence decay kinetics. The remaining elementary rate constants were determined by global fitting to the TRIR data with the criteria of minimizing the sum of the squared deviations between calculated and observed spectra (Figure S2), and producing component spectra consistent with the states involved in the reactions (Figure S3).

The final set of elementary rates constants used to generate calculated transient kinetics is:

$k_1 = 2.59 \times 10^{10} \text{ s}^{-1}$	$k_2 = 2.88 \times 10^9 \text{ s}^{-1}$	$k_3 = 2.04 \times 10^9 \text{ s}^{-1}$
$k_4 = 6.79 \times 10^8 \text{ s}^{-1}$	$k_5 = 3.27 \times 10^7 \text{ s}^{-1}$	$k_6 = 3.20 \times 10^5 \text{ s}^{-1}$
$k_7 = 7.70 \times 10^5 \text{ s}^{-1}$	$k_8 = 2.00 \times 10^7 \text{ s}^{-1}$	$K = 3$

Hopping Map

The two-step electron tunneling map was determined by solving the rate law corresponding to the following elementary reaction steps:



The elementary rate constants k_{XY} were defined in terms reaction driving force ($-\Delta G^\circ$), reorganization energy (λ), and donor-acceptor distance (r_{XY}) according to semiclassical electron-transfer theory (S11):

$$k_{\text{XY}} = \frac{\alpha}{\sqrt{\lambda_{\text{XY}} T}} \exp\{-\beta(r_{\text{XY}} - r_o)\} \exp\left\{-\frac{(\Delta G_{\text{XY}}^\circ + \lambda_{\text{XY}})}{4\lambda_{\text{XY}} RT}\right\}$$

where R is the gas constant, T is absolute temperature, and $\beta = 1.1 \text{ \AA}^{-1}$ is the empirical distance decay constant for electron tunneling through proteins (S11). The constant α is eliminated in analyses of the rate advantage of two-step vs. single-step tunneling.

The differential equations corresponding to this model were solved analytically using Mathematica 5.2 (Wolfram Research, Inc.). Two-step tunneling is strictly a biexponential process and one-step tunneling follows single-exponential kinetics. In order to compare the two, we defined an average electron transport time (τ) as follows:

$$F(t) = \frac{\mathbf{C}(t) - \mathbf{C}(\infty)}{\mathbf{C}(0) - \mathbf{C}(\infty)}; \quad \tau = \int_0^\infty F(t) dt$$

The relative advantage of two-step over single-step tunneling is defined as τ_{ET}/τ , where τ_{ET} is the time constant for single-step tunneling.

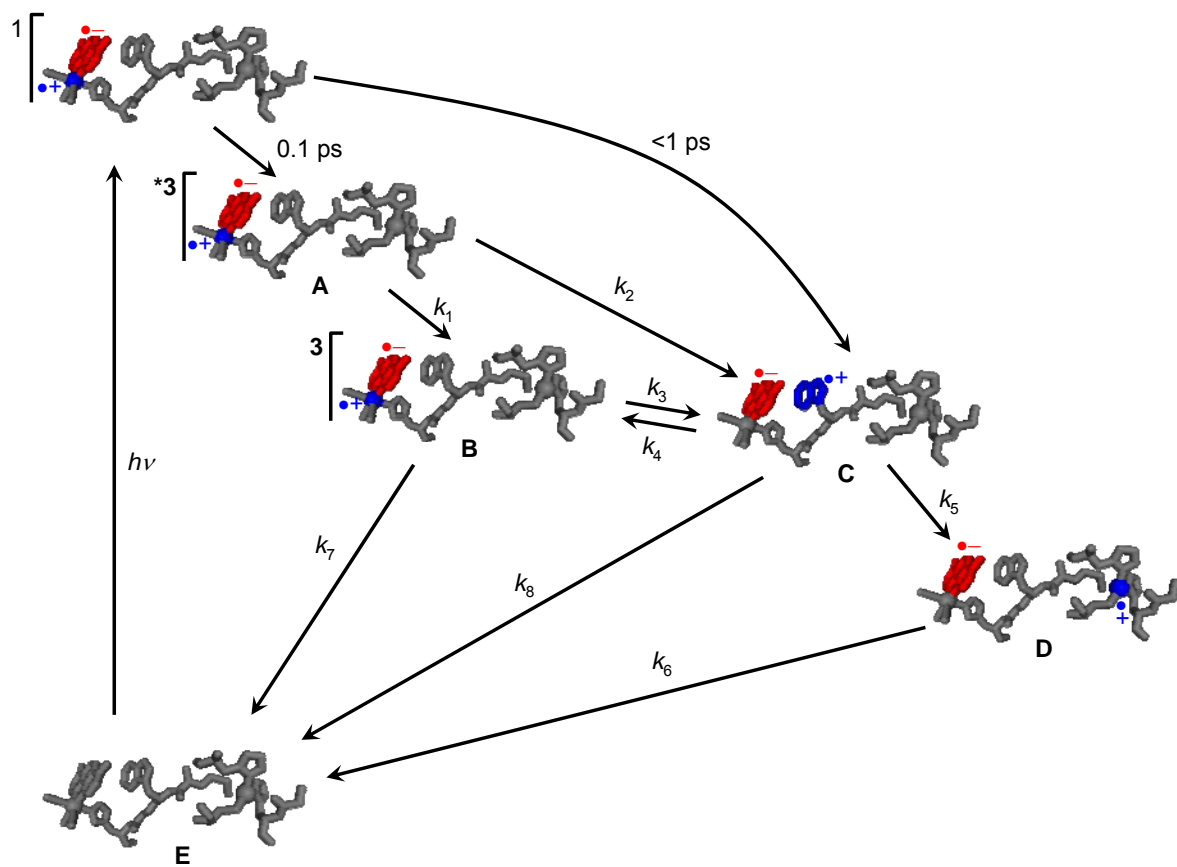


Figure S1. Reaction scheme used in kinetics modeling of photochemical electron transfer reactions in of $\text{Re}^{\text{I}}(\text{CO})_3(\text{dmp})(\text{H}^{124})|(\text{W}^{122})|\text{AzCu}^{\text{II}}$ (Az is azurin).

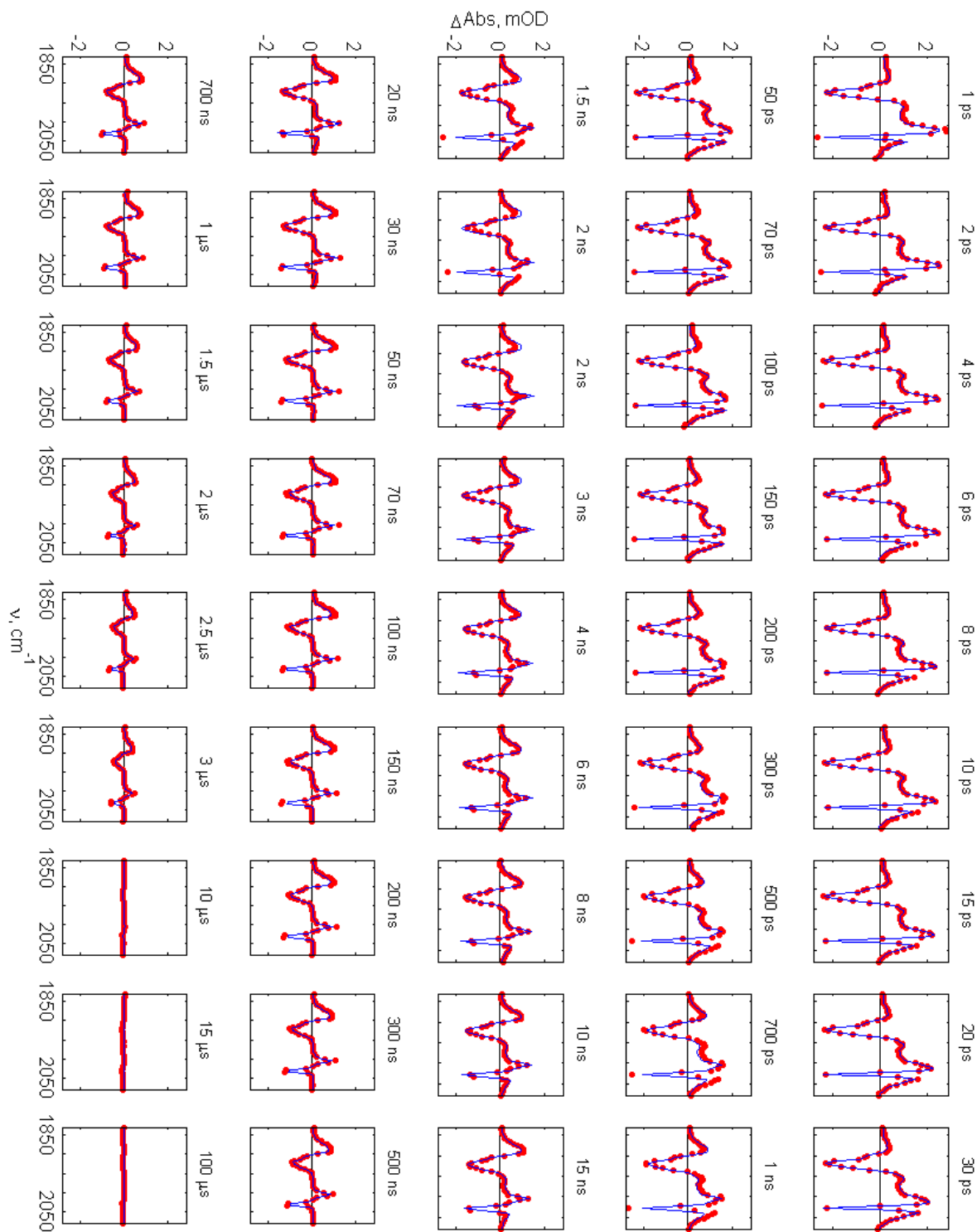


Figure S2. Experimental TRIR spectra (red) and calculated spectra (blue) based on the kinetics model and elementary rate constants described in the supporting text.

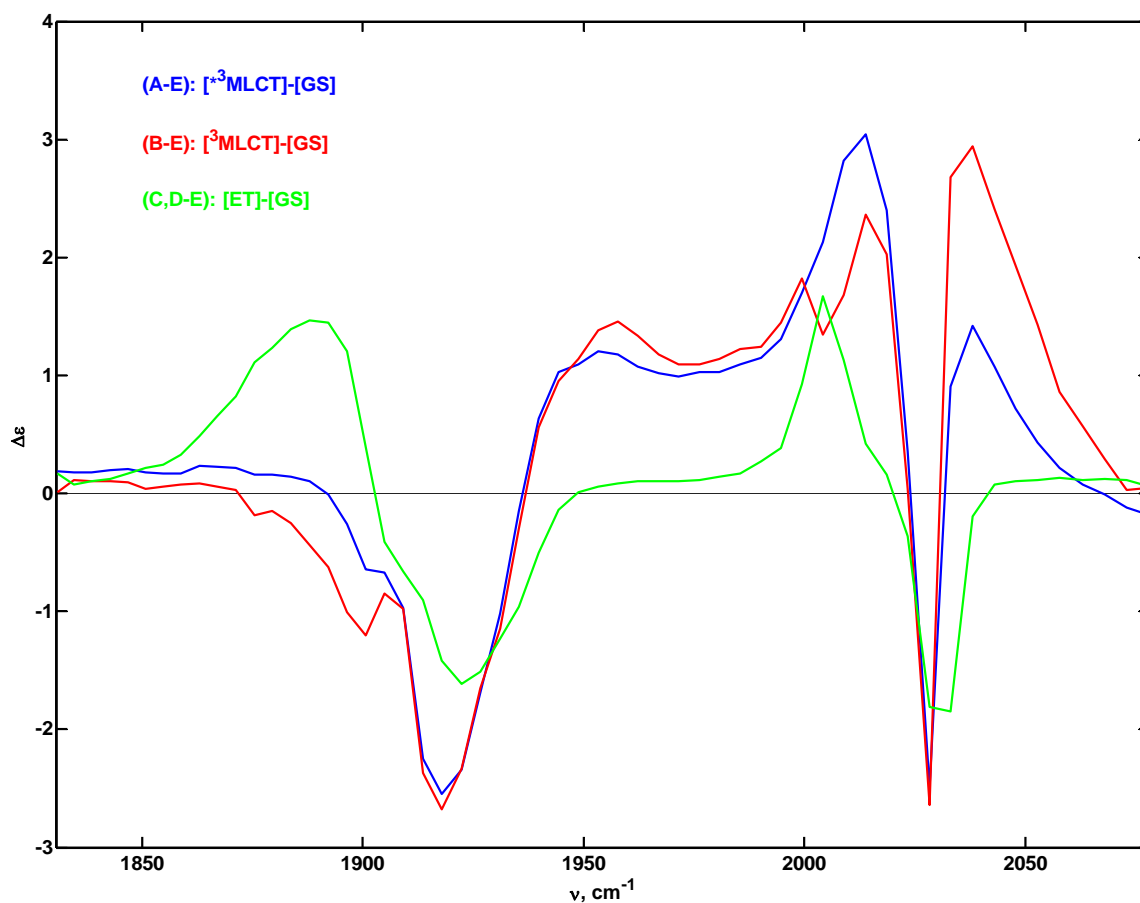


Figure S3. Component spectra used in fitting of the TRIR spectra using the kinetics model and elementary rate constants described in the supporting text. The blue spectrum is the vibrationally excited $^3\text{MLCT}$ state ($^3\text{Re}^{\text{II}}(\text{CO})_3(\text{dmp}^{\bullet-})(\text{H}^{124})$); the red spectrum is the equilibrated $^3\text{MLCT}$ state ($^3\text{Re}^{\text{II}}(\text{CO})_3(\text{dmp}^{\bullet-})(\text{H}^{124})$); and the green spectrum is the spectrum of the reduced Re complex ($\text{Re}^{\text{I}}(\text{CO})_3(\text{dmp}^{\bullet-})(\text{H}^{124})$).

Table S1. Data collection and refinement statistics for Re(4,7-dimethyl-1,10-phenanthroline)(CO)₃(H¹²⁴){T¹²⁴H|K¹²²W|H⁸³Q}(Cu^{II})azurin.

No. of residues	128
Ligand	Re(CO) ₃ (dmp)His ¹²⁴
number of waters	64
resolution (Å)	1.5 (1.50 – 1.55) ^g
number of unique reflections	24417
number of observations	344927
% completeness	99.6
$\langle I/\sigma I \rangle^a$	34.4 (8.4) ^g
R _{Sym} ^b (%)	8.2 (30.6) ^g
R ^c (%)	23.6 (28.5) ^g
R _{free} ^d (%)	25.5 (33.3) ^g
overall $\langle B \rangle^e$ (Å ²)	22.9
mainchain $\langle B \rangle$ (Å ²)	21.3
sidechain $\langle B \rangle$ (Å ²)	24.7
rmsd for bonds ^f (Å)	0.01
rmsd for angles ^f (degrees)	1.3

^a Intensity of the signal to noise ratio. ^b $R_{Sym} = \sum_j |I_j - \langle I \rangle| / \sum_j I_j$. ^c $R = \sum |F_{obs} - F_{calc}| / \sum F_{obs}$ for all reflections (no σ cutoff). ^d R_{free} calculated against 5% of reflections removed at random.

^e Overall model average thermal $\langle B \rangle$ factor. ^f Root mean square deviations from bond and angle restraints. ^g Highest resolution bin for compiling statistics

References

- S1. A. J. Di Bilio, B. R. Crane, W. A. Wehbi, C. N. Kiser, M. M. Abu-Omar, R. M. Carlos, J. H. Richards, J. R. Winkler, H. B. Gray *J. Am. Chem. Soc.*; **123**, 3181 (2001).
- S2. A. M. Blanco-Rodriguez, M. Busby, C. Grădinaru, B. R. Crane, A. J. Di Bilio, P. Matousek, M. Towrie, B. S. Leigh, J. H. Richards, A. Vlček, Jr., H. B. Gray *J. Am. Chem. Soc.*; **128**, 4365 (2006).
- S3. Z. Otwinowski, W. Minor, *Methods Enzymol.* **276** 307 (1997).
- S4. J. Navaza, *Acta Crystallogr.* **A50** 157 (1994).
- S5. Brunger *et al.*, *Acta Crystallogr.* **D54** 905 (1998).
- S6. D. E. McRee, *J. Mol. Graph.* **10** 44 (1992).
- S7. M. Towrie, D. C. Grills, J. Dyer, J. A. Weinstein, P. Matousek, R. Barton, P. D. Bailey, N. Subramaniam, W. M. Kwok, C. S. Ma, D. Phillips, A. W. Parker, M. W. George, *Appl. Spectrosc.* **57**, 367 (2003).
- S8. M. Towrie, A. W. Parker, A. Vlček, Jr., A. Gabrielsson, A. M. Blanco Rodriguez, *Applied Spectroscopy* **59**, 467 (2005).
- S9. D. Kuciauskas, M. S. Freund, H. B. Gray, J. R. Winkler, N. S. Lewis *J. Phys. Chem. B* **105**, 392 (2001).
- S10. J. C. Lee, R. Langen, P. A. Hummel, H. B. Gray, J. R. Winkler, *Proc. Natl. Acad. Sci. USA* **101**, 16466 (2004).
- S11. H. B. Gray, J. R. Winkler, *Quarterly Rev. Biophys.* **36**, 341 (2003).